

Binding of therapeutic Fc-fused factor VIII to the neonatal Fc receptor at neutral pH associates with poor half-life extension

Alejandra Reyes-Ruiz,¹ Sandrine Delignat,¹ Aishwarya Sudam Bhale,² Victoria Daventure,¹ Robin V. Lacombe,¹ Leslie Dourthe,¹ Olivier Christophe,³ Sune Justesen,⁴ Krishnan Venkataraman,² Jordan D. Dimitrov¹ and Sebastien Lacroix-Desmazes¹

¹Institut National de la Santé et de la Recherche Médicale, Centre de Recherche des Cordeliers, CNRS, Sorbonne Université, Université Paris Cité, Paris, France; ²Center for Bio-Separation Technology (CBST), Vellore Institute of Technology (VIT), Vellore, Tamil Nadu, India; ³Laboratory for Hemostasis, Inflammation and Thrombosis, Unité Mixte de Recherche 1176, Institut National de la Santé et de la Recherche Médicale, Université Paris-Saclay, Le Kremlin-Bicêtre, France and ⁴Immunitrack Aps, Copenhagen, Denmark

Correspondence: S. Lacroix-Desmazes
sebastien.lacroix-desmazes@inserm.fr

Received: August 30, 2024.
Accepted: December 5, 2024.
Early view: December 12, 2024.

<https://doi.org/10.3324/haematol.2024.286536>

©2025 Ferrata Storti Foundation

Published under a CC BY-NC license



Abstract

Fusion of therapeutic proteins to the Fc fragment of human immunoglobulin (Ig) G1 promotes their neonatal Fc receptor (FcRn)-mediated recycling and subsequent extension in circulating half-life. However, different Fc-fused proteins, as well as antibodies with different variable domains but identical Fc, may differ in terms of extension in half-life. Here we compared the binding behavior to FcRn of Fc-fused FVIII, Fc-fused FIX and two human monoclonal HIV-1 broadly-neutralizing IgG1, m66.6 and VRC01 with identical Fc. While all molecules bound FcRn at acidic pH, only rFVIII-Fc and m66.6 interacted with FcRn at neutral pH. *In silico* modeling predicted a role for charged residues in the C1 and C2 domains of FVIII, and in the variable domains of m66.6, in the neutral binding to FcRn. Accordingly, mutations of key positively charged amino-acids in the FVIII C1C2 domains decreased the binding of the protein to FcRn at pH 7.4 *in vitro* and increased the half-life of rFVIII-Fc in von Willebrand factor- knockout mice. Our findings suggest that the removal of positively charged patches on Fc-fused proteins to ameliorate FcRn recycling without affecting therapeutic efficacy, may improve their pharmacokinetic properties.

Introduction

Immunoglobulins (Ig) of the IgG isotype are among the circulating proteins with the longest half-life. IgG from humans, non-human primates and mice have half-lives of 7-21,¹ 8-9² and 6-8 days,³ respectively. Such long half-lives are mediated by binding of the “constant” crystallizable fragment (Fc) of the IgG to the neonatal Fc receptor (FcRn).⁴ Following pinocytosis, IgG reach early endosomes. Upon progressive acidification in the intra-endosomal space, the imidazole side chains of histidines in the IgG Fc fragments gain positive charges and promote the binding of the Fc I253, T254, H310, H433 and H435 residues to the negatively charged E115, E116, D130 and E133 residues of FcRn.⁵ Such interactions rescue IgG from lysosomal degradation and favor their recycling at the cell surface and release in the circulation at neutral pH.⁵ FcRn-mediated recycling of IgG was exploited as Fc-fusion technology to increase the half-life of therapeutic molecules with poor pharmacokinetics.⁶ Importantly, 79% of the Food and Drug Administration-ap-

proved Fc-fused molecules exhibit half-lives varying from 3 to 14 days.⁷⁻⁹

Coagulation factors VIII (FVIII) and IX (FIX) are two relevant examples of therapeutic proteins with short half-lives: 7 to 15 hours (h) with a mean of 11 h for FVIII and 29 to 44 h, with a mean of 36 h for FIX.¹⁰ FVIII and FIX are used as replacement therapy to restore coagulation in patients with hemophilia A (HA) or B (HB), two rare X-linked, recessive bleeding diseases caused by insufficient levels of endogenous FVIII or FIX, respectively. The poor pharmacokinetics of both therapeutic molecules impose twice to trice weekly dosing to ensure sufficient protein levels and optimal joint protection in patients with the severe forms of the disease.¹¹ In the last two decades, FVIII and FIX have been engineered by PEGylation,^{12,13} albumin-fusion¹⁴ or Fc-fusion technology^{15,16} in order to generate products with extended half-lives (EHL). While EHL FIX products achieve significantly longer half-lives (3- to over 5-fold) as compared to the unmodified short-half life (SHL) FIX products, the half-life extension of EHL FVIII products is

limited to 1.3- to 1.7-fold as compared to that of SHL FVIII products.¹⁰ Importantly, the limited half-life extension of therapeutic EHL FVIII ties patients with severe HA to life-long prophylactic treatment with dosing frequencies of two-times per week.¹⁵ The drastic differences in half-life extension observed between Fc-fused FVIII (rFVIII¹⁰Fc) and Fc-fused FIX (rFIX¹⁰Fc) suggest that both molecules are not recycled to similar extents by the FcRn. Interestingly, differences in pharmacokinetics have also been reported in the case of monoclonal human antibodies (mAb) that share identical Fc fragments but carry different variable (Fv) regions.¹⁷ Notably, the presence of positively charged amino acids in the Fv was found to affect FcRn-mediated recycling of some IgG; it favored interactions of the Fv with FcRn at neutral pH, thus preventing extracellular release and fostering lysosomal degradation.^{18,19}

The limited increase in half-life of rFVIII¹⁰Fc has so far been explained by the binding of the FVIII moiety of the therapeutic molecule to its endogenous chaperon, von Willebrand factor (VWF).²⁰ Under physiological conditions, the interaction of FVIII with VWF protects FVIII from uncontrolled activation and from interactions with FVIII-specific catabolic receptors.²¹⁻²³ It however favors the catabolism of the FVIII/VWF complex by VWF-specific receptors.²⁴ Yet, additional VWF-independent mechanisms may contribute to limitation in FVIII half-life extension. Indeed, a Fc-fused FVIII that includes the FVIII-binding D'D3 domains of VWF and free FVIII from its dependence on endogenous VWF did not demonstrate increased half-life in von Willebrand factor-knockout (VWF-KO) mice;²⁵ the 35 hour-long half-life of efanesoctocog α was only achieved following introduction of XTEN polypeptides in the molecule.²⁵

Here, we investigated whether other mechanisms beyond VWF catabolism could contribute to the short half-life of rFVIII¹⁰Fc. We observed that rFVIII¹⁰Fc binds FcRn at neutral pH. The binding was associated with the presence of positively charged residues in the C1 and C2 domains of the FVIII moiety of the molecule. Mutations of key charged amino acids drastically reduced the binding of rFVIII¹⁰Fc to FcRn at neutral pH. It further led to a 2.5-fold increased half-life in VWF-deficient mice.

Methods

Sources of Fc-fused molecules

Recombinant Fc-fused FIX (Alprolix[®]), B domain-deleted (BDD) FVIII (ReFacto AF[®]) and Fc-fused BDD-FVIII (rFVIII¹⁰Fc, Eloctate[®]) were gifts from Sanofi-Genentech and SOBI. The rFVIII^{C1C2}Fc. rFVIII^{N2118Q}Fc mutants were generated by site-directed mutagenesis applying In-Fusion system (Takara) using the cDNA encoding human BDD-FVIII (containing the SFSQNPPVLKRHRQR segment instead of the B domain), and the cDNA encoding a human Fc γ 1 domain dimerized with a linker (provided by Sanofi[®]) as templates. The mutated

cDNA were cloned in the ReNeo plasmid and validated by standard sequencing analysis. The rFVIII^{C1C2}Fc mutant bears the R2090A, K2092A, F2093A, R2215A mutations. BHK-M cells were transfected and selected for neomycin-resistant clones using Geneticin-sulfate (500 μ g/mL, Sigma-Aldrich, St. Louis, MO). FVIII producing clones were screened using a FVIII chromogenic assay (Siemens Healthcare, Erlangen, Germany). The selected highest expressing clones were scaled up to near confluency before switching the medium to serum-free AIM-V medium (Thermo Scientific, Waltham, MA). Medium was collected every 24 h; cells were replenished with fresh AIM-V medium. FVIII purification was performed by affinity chromatography on VIIIselect column (GE Healthcare, Chicago, IL), followed by anion-exchange chromatography on HiTrap Resource Q column (GE Healthcare). Purified rFVIII¹⁰Fc was analyzed by 4-12% SDS-PAGE \pm activation by bovine thrombin (Sigma-Aldrich) (*Online Supplementary Figure S1*) and detected by silver staining. The activity of the different purified rFVIII¹⁰Fc variants was measured using the FVIII chromogenic assay; protein concentrations were measured using nanodrop or Bradford assay (Bio-Rad, Hercules, CA) (*Online Supplementary Table S1*). The specific activities were 4,265 IU/mg for rFVIII¹⁰Fc, 1,392 to 2,398 IU/mg for FVIII^{C1C2}Fc and 1,951 IU/mg for FVIII^{N2118Q}Fc (*Online Supplementary Table S1*). The study has been approved by a formally constituted review board (Charles Darwin ethics committee #28694-2020121017336521).

Results

Fc-fused FVIII binds to FcRn at physiological pH

The commercially available Fc-fused B domain-deleted (BDD) FVIII (Eloctate[®]) presents with a limited increase in FVIII half-life over therapeutic BDD FVIII as compared to human IgG and other therapeutic Fc-fused molecules, thus raising questions on its capacity to be recycled by the FcRn following endocytosis. Using real time interaction analyses based on surface plasmon resonance (SPR) (see the *Online Supplementary Appendix*), we first confirmed that, at pH 6, rFVIII¹⁰Fc interacts with human and murine FcRn with binding affinities (1.4-2.0 and 0.2-0.3 nM, respectively; Table 1) similar to that measured for m66.6 (1.3-2.8 and 0.2-0.4 nM), a human anti-MPER HIV monoclonal IgG.²⁶ The affinities were slightly higher than that determined for commercially available Fc-fused FIX (rFIX¹⁰Fc, Alprolix[®], 2.1-5.0 and 0.3-0.9 nM, respectively)²⁷ and VRC01 (3.1-5.0 and 0.4-0.9 nM, respectively), a human monoclonal IgG specific for HIV gp120²⁸ (Figure 1A, B). These results were confirmed by enzyme-linked immunosorbent assay (ELISA). At acidic pH, rFVIII¹⁰Fc, rFIX¹⁰Fc, m66.6 and VRC01 exhibited similar binding profiles to human or mouse FcRn (Figure 1C). At neutral pH however, rFVIII¹⁰Fc and m66.6 presented with residual binding to both human and mouse FcRn that was greater than that observed for rFIX¹⁰Fc and VRC01 (Figure 2A, B). By

ELISA, rFVIII-Fc and m66.6 IgG bound to human and mouse FcRn at pH 7.4 in a dose-dependent manner, while rFIX-Fc and VRC01 exhibited a weak binding (Figure 2C). The binding of BDD-FVIII without the Fc fragment to human and mouse FcRn, that was not detected by SPR at pH 7.4 (Figure 1C), was evidenced by ELISA with a 50% binding close to 1,140 and 130 nM, respectively (*Online Supplementary Figure S2*).

The C1 and C2 domains of FVIII exhibit a largely positive electrostatic potential

Modeling of the charge distribution on the Fab fragments of m66.6 and VRC01 highlighted a strong positive electrostatic potential for m66.6 (Figure 3A), that was not present in the case of VRC01 (Figure 3B). Positive charges in the Fv of some human monoclonal IgG have been implicated in their binding to the FcRn at neutral pH and poor pharmacokinetics.^{18,19} Our results are in accordance with the latter finding since the presence of positive charges in the Fab fragment of m66.6 was associated with important residual binding to human and mouse FcRn (Figure 2). To get insight into potential reasons for the residual binding of rFVIII-Fc to FcRn at neutral pH, we modeled the charge distribution on BDD-FVIII and FcRn. FVIII is a multidomain protein formed of a heavy chain containing the A1a1, A2a2 and B domains, and a light chain containing the a3A3, C1 and C2 domains (*Online Supplementary Figure S3A*).²⁹ In BDD-FVIII, the C1 and C2 domains exhibited a highly positive electrostatic potential (Figure 2C), as well as a portion of the A3 domain albeit to a lesser extent, reminiscent of the situation with m66.6 Fab (Figure 2A). In contrast, the surface electrostatic potential of FcRn was predominantly negative (Figure 3D), making it an ideal binding partner for the C1 and C2 domains of FVIII.

Charged residues in the FVIII C1 and C2 domains are predicted to promote binding to FcRn

To decipher whether the charge distribution in rFVIII-Fc and m66.6 governs binding to FcRn at neutral pH, we studied the effect of variations in ionic strength on FcRn binding by ELISA. The interaction of both molecules with human and mouse FcRn was inhibited in a dose-dependent manner by NaCl concentrations above the physiological value (i.e., 140 mM) and increased with decreasing NaCl concentrations (Figure 4A). As expected, VRC01 and rFIX-Fc showed a lower binding to FcRn than rFVIII-Fc and m66.6, irrespective of the salt concentration. To confirm the implication of the C1 and C2 domains in the binding of rFVIII-Fc to FcRn at neutral pH, we measured, by real time interaction analyses at pH 7.4, the binding to FcRn of rFVIII-Fc pre-incubated alone, with VWF to mask its light chain, or with the F(ab')₂ fragments of the human monoclonal anti-FVIII IgG KM33, BO2C11, and BO1B2, that recognize epitopes in the C1,³⁰ C2³¹ and A2 (patent US20070065425A1) domains of FVIII, respectively. Of note, rFVIII-Fc retained unperturbed binding to VWF as compared to rFVIII by ELISA (*Online Supplementary Figure S4A*). Shielding of rFVIII-Fc with VWF almost completely abrogated binding of rFVIII-Fc to FcRn (Figure 4B). The protecting effect of VWF was reproduced independently by the anti-C1 and anti-C2 F(ab')₂ fragments, confirming the contribution of residues in the latter domains to the binding of rFVIII-Fc to FcRn at neutral pH. In contrast, the anti-A2 F(ab')₂ fragments did not interfere with rFVIII-Fc binding to FcRn (Figure 4B). The independent FVIII^{C1} and FVIII^{C2} variants containing three mutations in the C1 domain (R2090A, K2092A, F2093A) and one or two mutations in the C2 domain (R2215A and/or R2220A), respectively, lose binding to their cognate antibodies KM33 and BO2C11.^{32,33} *In silico* molecular modeling

Table 1. Kinetic parameters for the binding of Fc-fused molecules or antibodies to human and mouse FcRn at pH 6.

	<i>k_a</i> (M ⁻¹ .s ⁻¹)	<i>k_d</i> (s ⁻¹)	<i>K_d</i> (nM)	χ ²
Binding to human FcRn				
rFVIII-Fc	1.6-2.7x10 ⁶	3.4-3.7x10 ⁻³	1.4-2.0	<9.0
rFIX-Fc	1.0-1.6x10 ⁶	3.0-8.0x10 ⁻³	3.1-5.0	>5.0
m66.6	1.5-2.0x10 ⁶	2.0-4.2x10 ⁻³	1.3-2.8	<14
VRC01	0.7-1.9x10 ⁶	2.5-6.1x10 ⁻³	3.1-5.1	<12
Binding to murine FcRn				
rFVIII-Fc	1.0x10 ⁶	2.3-2.8x10 ⁻⁴	0.2-0.3	<3.4
rFIX-Fc	0.25-1.4x10 ⁶	2.3-6.2x10 ⁻⁴	0.3-0.9	<8.0
m66.6	0.9-1.3x10 ⁶	2.0-3.9x10 ⁻⁴	0.2-0.4	<14
VRC01	5.4-6.4x10 ⁵	2.8-5.7 x10 ⁻⁴	0.4-0.9	<2.4

The binding kinetics of the different Fc-fused molecules and antibodies were calculated by surface plasmon resonance at pH 6 after injection of serial dilutions of Fc-fused molecules or antibodies (flow, 30 μL/minute; volume, 120 μL; dissociation time, 300 seconds) in streptavidin-coated chips with immobilized biotinylated human or mouse FcRn at 500 RU. The values are represented as the range of 2 or 3 independent experiments. Fc: “constant” crystallizable fragment; FcRn: neonatal Fc receptor; FVIII: coagulation factor VIII; FIX: coagulation factor IX.

of a FVIII^{C1C2} mutant combining the four mutations (R2090A, K2092A, F2093A, R2215A) suggested that the removal of three positively charged residues in the FVIII C1 and C2 domains strikingly decreases the positive electrostatic potential of the FVIII light chain (Figures 3C and 4C). To further predict the role of these amino acid residues in the interaction, we conducted domain-specific docking of the C1C2 domain of FVIII to FcRn at neutral pH using the modeled structure of C1C2 (*Online Supplementary Figure S3*) and the HDOCK webserver. The docking yielded a binding score of -282.48, a confidence score of 0.9340, and a ligand

RMSD of 124.49 Å. The interaction analysis identified the formation of four hydrogen bonds, two salt bridges, and 204 non-bonded contacts that could be either hydrophobic, van der Waals or electrostatic interactions between the C1C2 domains and FcRn (Figure 4D). Specifically, within the C1 domain, C2021 formed a hydrogen bond with N55 of FcRn, and R2090 formed hydrogen bonds with S181 and P180 of FcRn (Table 2). Within the C2 domain, K2207 formed a hydrogen bond with D101 of FcRn. Additionally, two residues from the C2 domain were involved in salt bridge formation: E2181 with R171 of FcRn and K2207 with D101 of FcRn (Ta-

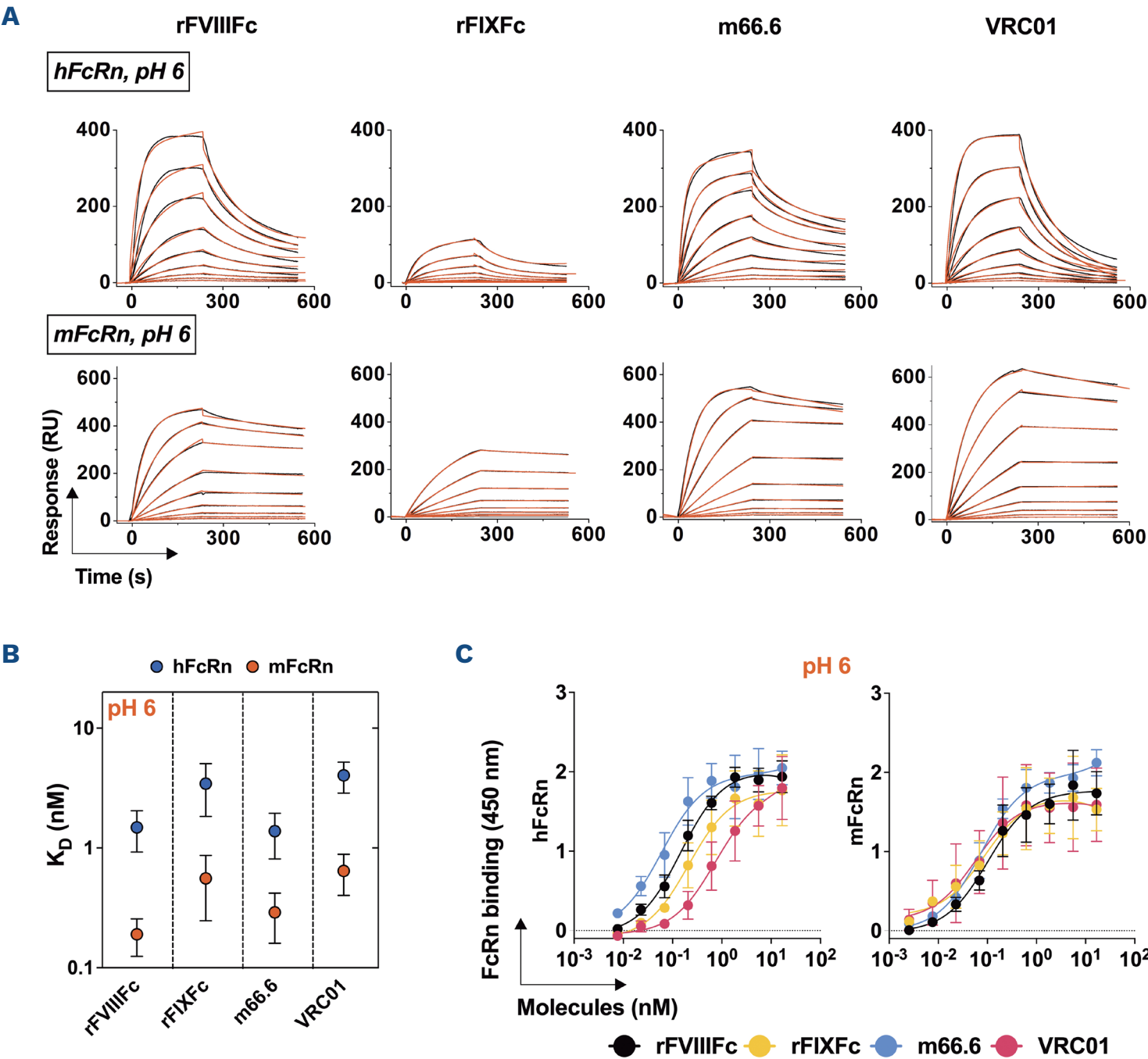


Figure 1. rFVIII^{C1C2} binds to FcRn at acidic pH. (A) Real-time interaction profiles of binding of rFVIII^{C1C2}, FIX^{C1C2}, m66.6 or VRC01 to immobilized human (top) or murine (bottom) FcRn at pH 6. The black line depicts the binding profiles obtained after injection of serial dilutions of Fc-fused molecules or antibodies (25 to 0.097 nM). The red lines depict the fits of data obtained by global analysis using Langmuir kinetic model. (B) Values of the equilibrium dissociation constants calculated from the values of association and dissociation rate constants ($K_D = K_d / K_a$) for the binding of rFVIII^{C1C2}, FIX^{C1C2}, m66.6 or VRC01 to human (blue) or murine (red) FcRn at pH 6 (Table 1). The graphs depict means \pm standard deviation (SD) (N=2 or 3). (C) Binding of rFVIII^{C1C2}, FIX^{C1C2}, VRC01 “trastuzumab” by m66.6 to human (left) or murine (right) FcRn by enzyme-linked immunosorbent assay at pH 6. The Fc-fused molecules or antibodies were incubated in serial dilutions on plates coated with FcRn. The graphs depict the binding of the Fc-fused proteins or antibodies detected using a horseradish peroxidase conjugated anti-human immunoglobulin Fc antibody. Binding is expressed as arbitrary units (AU) as mean \pm SD based on the optical density measured at 450 nm in 2 independent experiments. Fc: “constant” crystallizable fragment; FcRn: neonatal Fc receptor; FVIII: coagulation factor VIII; FIX: coagulation factor IX.

ble 2). Furthermore, in the C1 domain, R2090, K2092 and F2093 formed non-bonded contacts with P179, P180, S181 and M182, with R183, and with R183 of FcRn, respectively. In the C2 domain, R2215 formed a non-bonded contact with P100 of FcRn. From the FcRn residues predicted to interact with C1 and C2, W53 (*Online Supplementary Table S1*; Table 2; Figure 4D) was shared with the central residues contributing to albumin interaction.³⁴ None of the latter residues was shared with the IgG binding site (Figure 4D).⁵

Binding of rFVIII^h to FcRn at neutral pH is mediated by the FVIII C1 and C2 domains

To confirm the importance of the C1 and C2 residues in the interaction with FcRn at neutral pH, we produced

a rFVIII^{C1C2}Fc mutant molecule containing the R2090A, K2092A, F2093A mutations in the C1 domain and the R2215A mutation in the C2 domain. As a control, we produced a rFVIII^{N218Q}Fc mutant wherein the N-glycosylation site in the C1 domain is removed.³⁵ In the rFVIII^{C1C2}Fc and rFVIII^{N218Q}Fc mutants, the Fc fragments are stabilized by a (GGGGS)₄ linker. Hence, the migration profile of the molecules slightly differed from that of rFVIII^hFc, both when incubated alone and in the presence of thrombin (*Online Supplementary Figure S1*). Besides, the specific activities of rFVIII^{C1C2}Fc (1,392–2,398 IU/mg; *Online Supplementary Table S2*) and rFVIII^{N218Q}Fc (1,951 IU/mg) were lower than that of rFVIII^hFc (4,265 IU/mg). Both rFVIII^{C1C2}Fc and rFVIII^{N218Q}Fc retains unperturbed binding to VWF (*Online Supplementary Fig-*

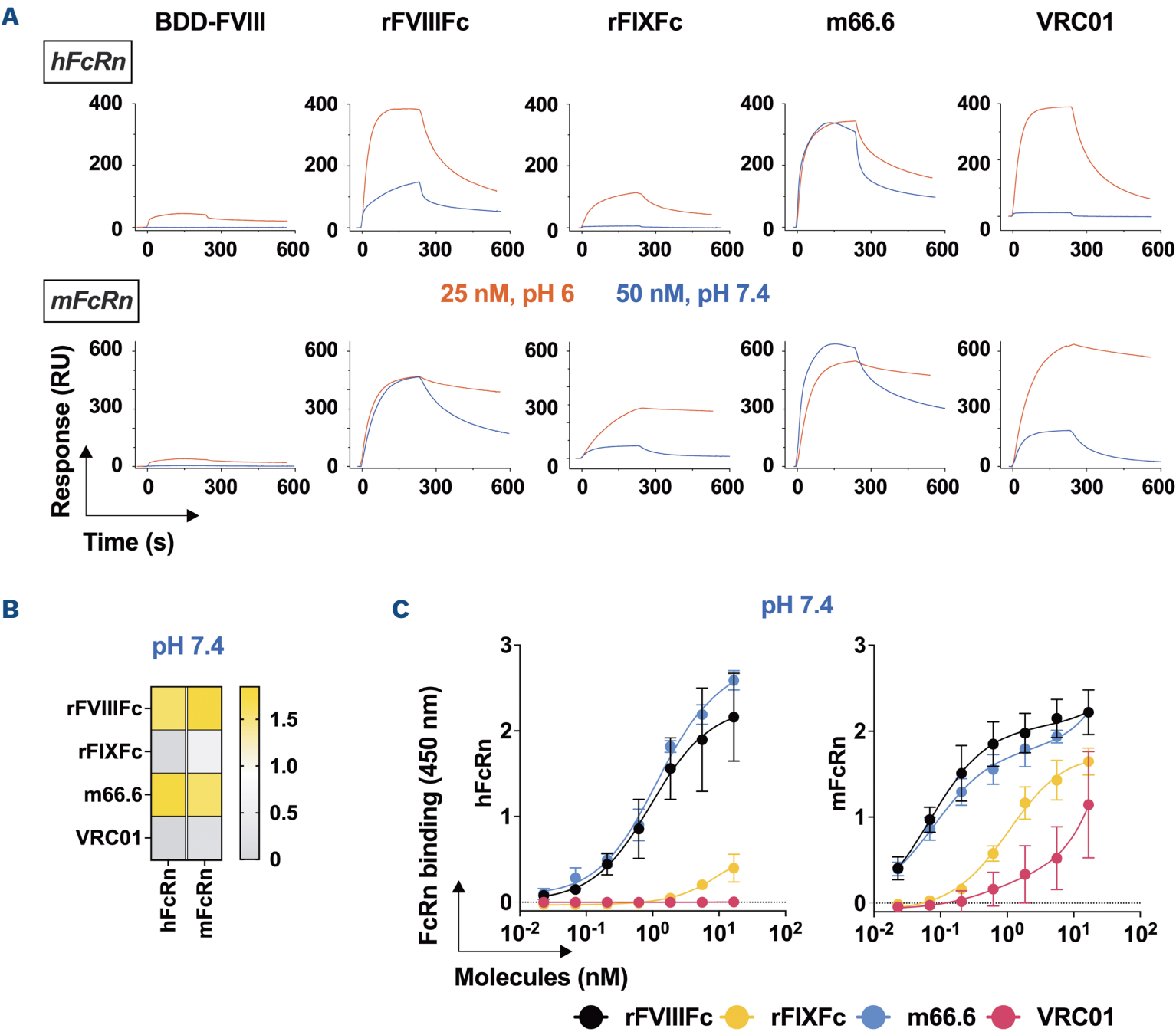


Figure 2. rFVIII^h shows a residual binding to FcRn at neutral pH. (A) Sensorgrams of BDD-FVIII, rFVIII^hFc, FIXFc, m66.6 or VRC01 binding to immobilized human (top) or murine (bottom) FcRn at pH 6 (red curves) or pH 7.4 (blue curves). Molecules were injected at 25 nM or 50 nM for pH 6 and pH 7.4, respectively. (B) Heatmap showing the binding intensity of rFVIII^hFc, FIXFc, m66.6 or VRC01 to human or murine FcRn at pH 7.4 by enzyme-linked immunosorbent assay (ELISA). (C) Binding of rFVIII^hFc, FIXFc, VRC01 “trastuzumab” by m66.6 to human (left) or murine (right) FcRn by ELISA at pH 7.4. The Fc-fused molecules or antibodies were incubated in serial dilutions on plates coated with FcRn. The graphs depict the binding of the Fc-fused proteins or antibodies detected using a horseradish peroxidase-conjugated anti-human immunoglobulin (Ig) Fc antibody. Binding is expressed as arbitrary units (AU) as mean \pm SD based on the optical density measured at 450 nm in 2 independent experiments. Fc: “constant” crystallizable fragment; FcRn: neonatal Fc receptor; FVIII: coagulation factor VIII; FIX: coagulation factor IX; rFVIII^hFc: Fc-fused FVIII.

ure S4A), reflecting the relative integrity of the light chain structure in the mutated molecules. At pH 6, rFVIII^{N2118Q}Fc and rFVIII^{C1C2}Fc demonstrated similar binding affinities for FcRn (Figure 5A; *Online Supplementary Table S3*) as assessed by SPR-based kinetics analyses. The affinities were similar to that determined for rFVIII^{FC}Fc (Table 1), suggesting that not all three charged residues contribute to the interaction with FcRn. In agreement, binding ELISA performed at pH 6, revealed identical binding profiles for the three molecules towards mouse and human FcRn (*On-*

line Supplementary Figure S4B). These data suggest that stabilization of the Fc fragments with a linker, removal of the N-linked glycan in FVIII^{N2118Q}Fc or introduction of mutations in the C1 and C2 domains of rFVIII^{C1C2}Fc do not alter binding to FcRn in acidic conditions. While, at neutral pH, FVIII^{N2118Q}Fc retained the same binding behavior to FcRn as rFVIII^{FC}Fc, the rFVIII^{C1C2}Fc mutant demonstrated significantly decreased FcRn binding (Figure 5B, C). Similarly, the rFVIII^{C1C2}Fc mutant did not bind to FcRn at neutral pH, irrespective of the salt concentration (Figure

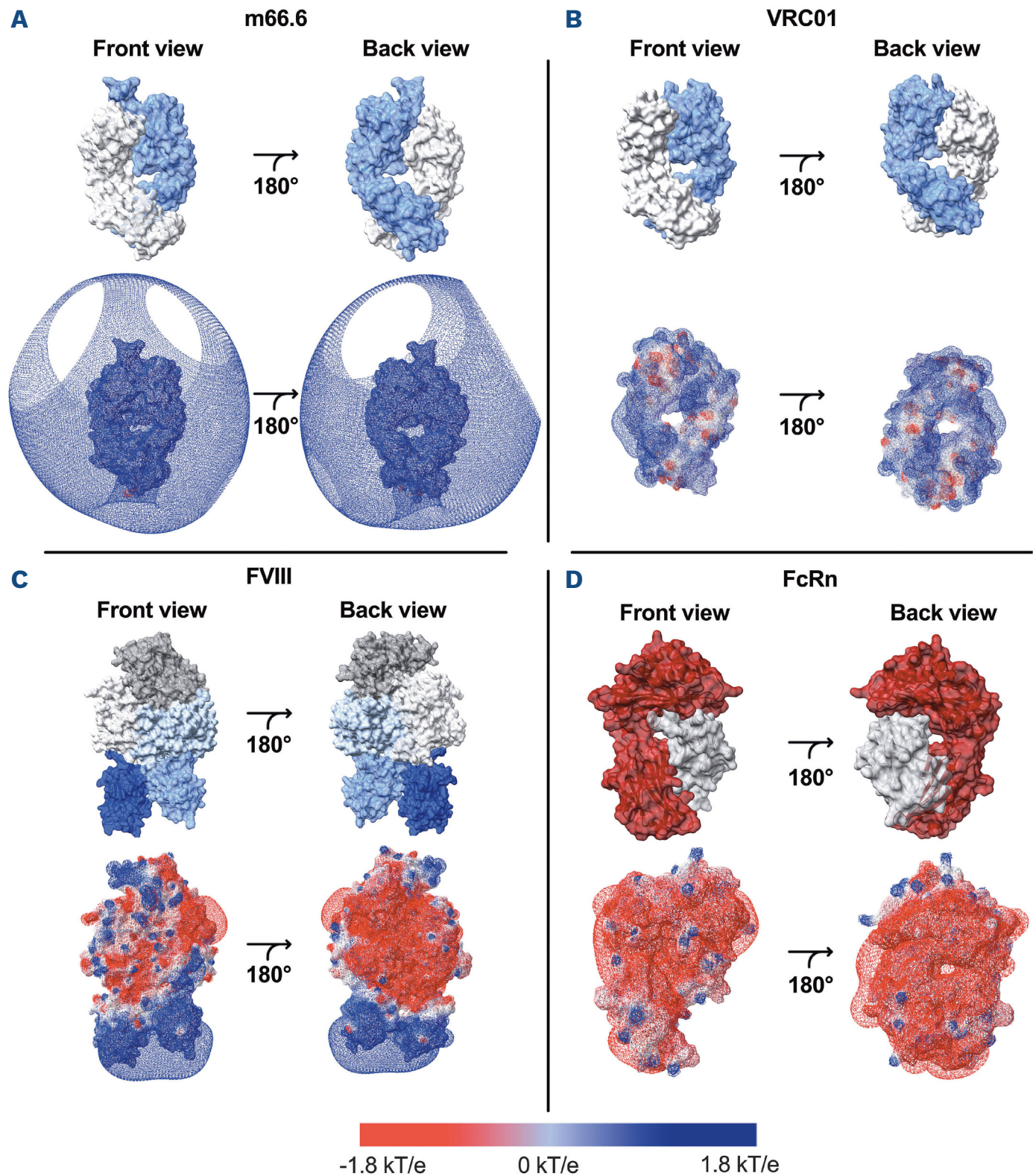


Figure 3. The light chain of FVIII exhibit a positive electrostatic potential at neutral pH. (A) Structure of human anti-HIV m66.6 Fab (PDB: 4NRZ) and (B) of human anti-HIV VRC01-class DRVIA7 Fab (PDB: 5CD5). The heavy (VH-CH1) and light chains (VL-CL) of the human Fabs are depicted in cyan and white, respectively. (C) BDD FVIII structure (PDB: 6MF2). The FVIII A1, A2, A3, C1 and C2 domains are depicted in white, gray, light blue, cyan and cobalt blue, respectively. (D) Structure of human FcRn (PDB: 4N0F). The heavy chain of FcRn is depicted in red and the light chain $\beta 2$ macroglobulin in light gray. The surface electrostatic potentials calculated using the Coulomb method (SWISS-PDB viewer) are shown at the bottom of each structure. Negative potentials are depicted in red and positive potentials in blue. Fc: “constant” crystallizable fragment; FcRn: neonatal Fc receptor; FVIII: coagulation factor VIII.

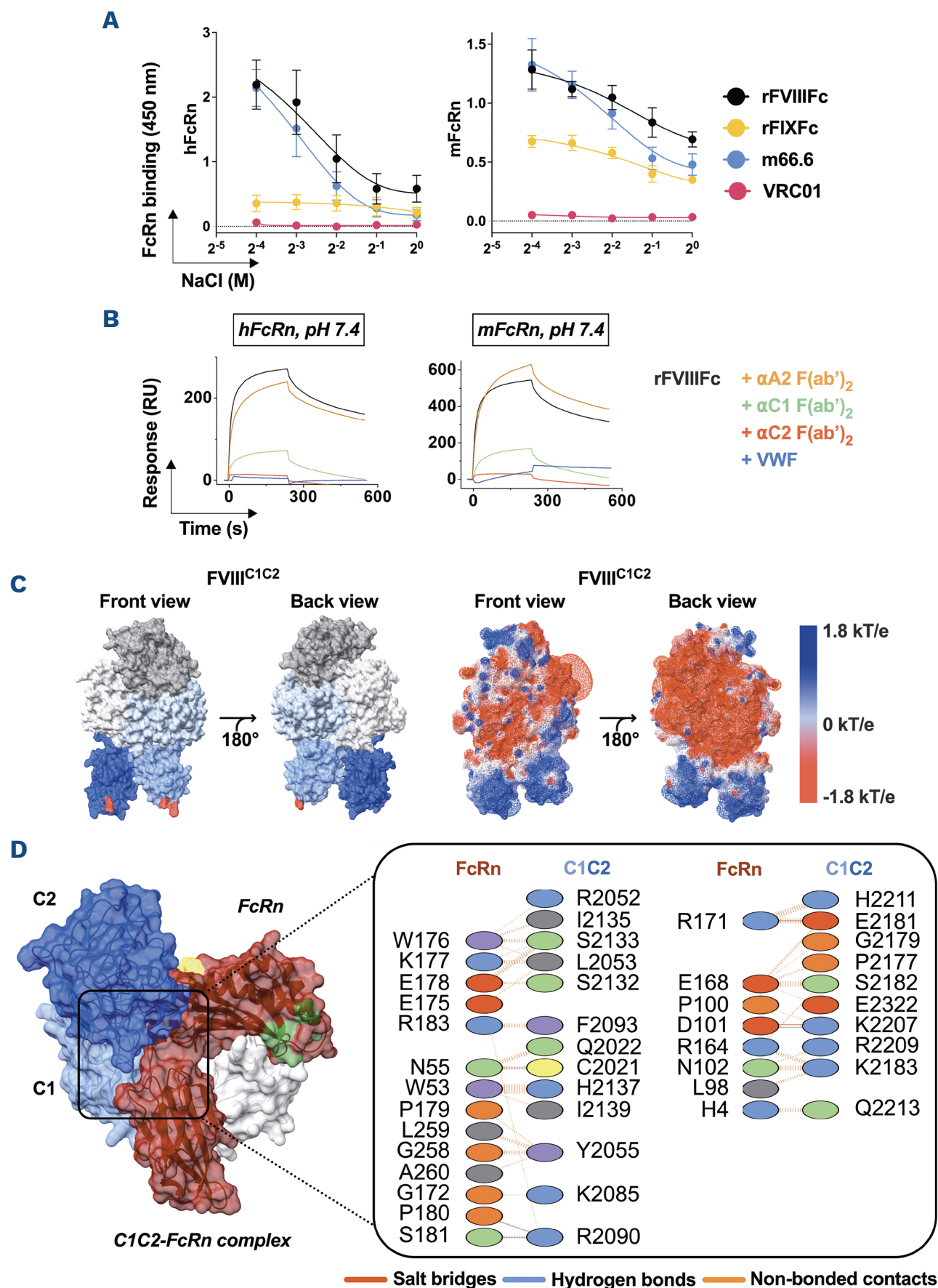


Figure 4. Positively charged residues in the C1 and C2 domains of rFVIII^{C1C2} mediate the binding of rFVIII^{C1C2} to FcRn at neutral pH. (A) The ionic strength dependence of the binding of Fc-fused molecules and antibodies to FcRn was evaluated by enzyme-linked immunosorbant assay (ELISA). Error bars indicate the standard deviation (SD) of 6 OD_{450 nm} values. (B) Sensorgrams of the binding of rFVIII^{C1C2} alone (black curve), rFVIII^{C1C2} pre-incubated with the F(ab')₂ fragment of the anti-A2 IgG BOIIB2 (orange curve), of the anti-C1 IgG KM33 (green curve), of the anti-C2 IgG BO2C11 (red curve), or with von Willebrand factor (VWF) (blue curve) to immobilized human (left) or murine (right) FcRn at pH 7.4. (C) Structure of the modeled human BDD FVIII (PDB: 6MF2) with 4 mutations at positions: R2090A, K2092A, F2093A, R2215A (FVIII^{C1C2}). The FVIII A1, A2, A3, C1 and C2 domains are depicted in white, gray, light blue, cyan and cobalt blue, respectively. Mutated residues are highlighted in red. The surface electrostatic potential of the FVIII^{C1C2} mutant calculated using the Coulomb method (SWISS-PDB viewer) is shown on the right. (D) Protein-protein interaction of C1C2 and FcRn utilizing the HDock webserver. Protein structures were refined at pH 7.4 using PROPKA3.1, ProteinPrepare. The illustration shows the docked complex of C1C2 domains of FVIII in cyan and cobalt blue, respectively and FcRn containing the heavy chain depicted in red and the light chain β 2 macroglobulin in light gray. Amino acids from FcRn that are important for the Fc interaction at acidic pH (E115, E116, D130 and E133) are highlighted in green, while central amino-acids for albumin binding (W53, W59, S58, H161, H166) are highlighted in yellow. Amino acids from FcRn and C1C2 domains that are important for binding are shown on the right. Positive (H, K, R) residues are depicted in blue; negative (D, E) in red; neutral (S, T, N, Q) in lime; aliphatic (A, V, L, I, M) in gray, aromatic (F, Y, W) in purple, proline and glycine in orange, and cysteine in yellow. Fc: “constant” crystallizable fragment; FcRn: neonatal Fc receptor; FVIII: coagulation factor VIII; FIX: coagulation factor IX; rFVIII^{C1C2}: Fc-fused FVIII.

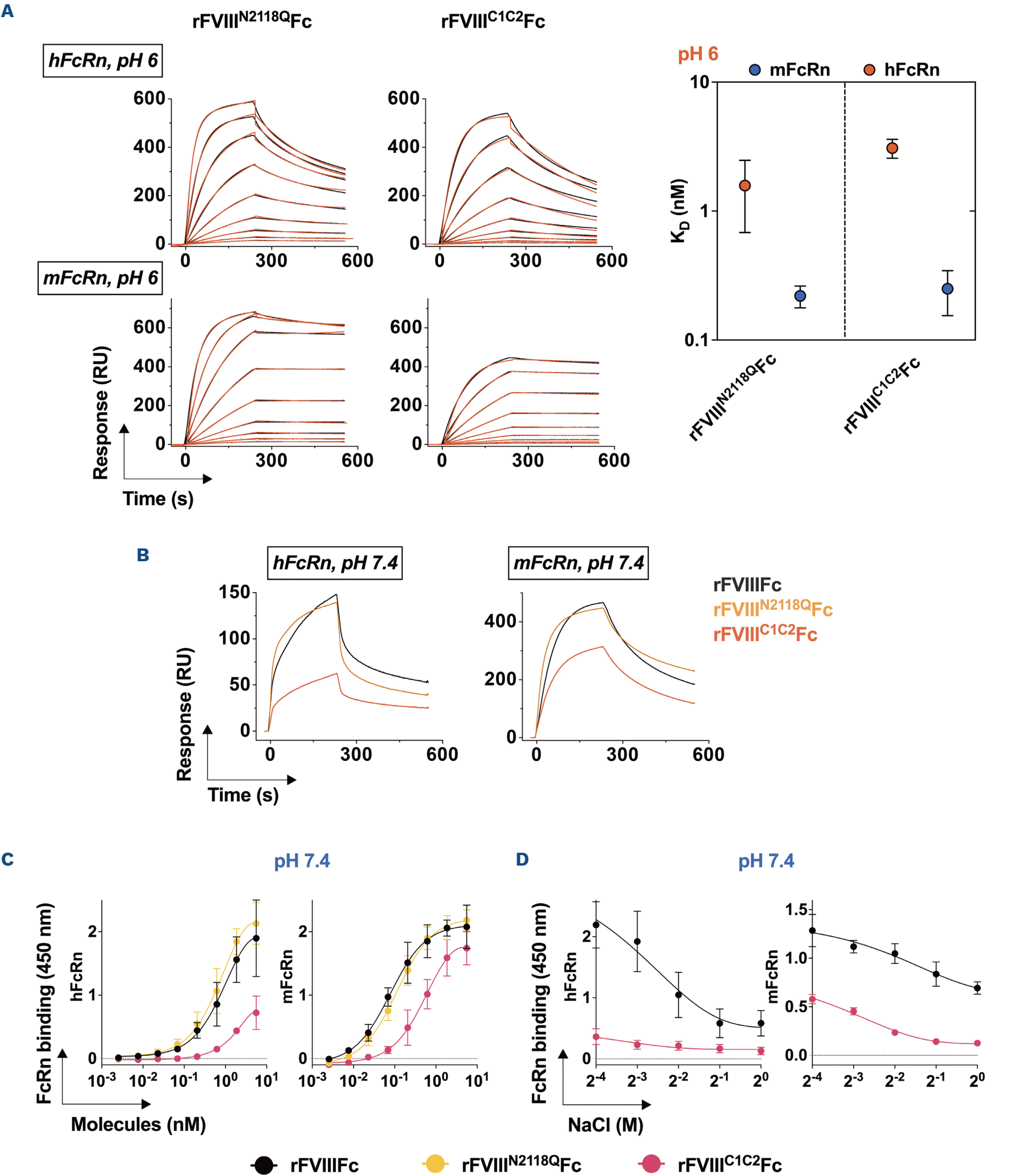


Figure 5. Mutations in the C1 and C2 domains of FVIII moiety in rFVIII^hFc decrease the binding to FcRn at neutral pH. (A) Real-time interaction profiles of FVIII^{N2118Q}Fc or FVIII^{C1C2}Fc with immobilized human (top) or murine (bottom) FcRn at pH 6. The black line depicts the binding profiles obtained after injection of serial dilutions of the rFVIII^hFc variants (25 to 0.097 nM). The red lines depict the fits of data obtained by global analysis using Langmuir kinetic model. The values of the equilibrium dissociation constants calculated from the values of association and dissociation rate constants ($K_D=K_d/K_a$) for the binding of FVII-

Continued on following page.

I^{N2118Q}Fc or FVIII^{C1C2}Fc to human (blue) or murine (red) FcRn at pH 6 are depicted in the graph on the right (Table 1). (B) Sensorgrams of the binding of rFVIII^Q (black curve), FVIII^{N2118Q} (orange curve) or FVIII^{C1C2} (red curve) to immobilized human (left) or murine (right) FcRn at pH 7.4. (C) Binding of rFVIII^Q or rFVIII^Q variants (0.0025–5.5 nM) to human (left) or murine (right) FcRn by enzyme-linked immunosorbent assay (ELISA) at pH 7.4. The Fc-fused molecules were incubated in serial dilutions on plates coated with FcRn. (D) Ionic strength dependence of the binding of Fc-fused FVIII variants to human (left) or murine (right) FcRn evaluated by ELISA. The graphs depict the binding of the Fc-fused proteins detected using a secondary goat F(ab')₂ anti-human Ig Fc conjugated to horseradish peroxidase. Binding is expressed as arbitrary units (AU) as mean ± standard deviation (SD) based on the optical density measured at 450 nm in 2 independent experiments. Fc: “constant” crystallizable fragment; FcRn: neonatal Fc receptor; FVIII: coagulation factor VIII; FIX: coagulation factor IX; rFVIII^Q: Fc-fused FVIII.

5D), in contrast to rFVIII^Q. Together, the data confirm the contribution of positively charged residues in the FVIII C1 and C2 domains to FcRn binding at physiological pH.

Mutations of charged residues in the C1 and C2 domains of rFVIII^Q increase its half-life in von Willebrand factor-knockout mice

We then evaluated the half-lives of wild-type rFVIII^Q and the engineered FVIII^{C1C2}Fc in mice. The binding of rFVIII^Q to endogenous VWF has been shown to contribute for the largest part to the limited extension in half-life, owing to elimination of the rFVIII^Q/VWF complex by VWF-specific catabolic receptors.²⁵ In agreement with this, rFVIII^Q and FVIII^{C1C2}Fc exhibited comparable pharmacokinetics in FVIII-KO mice, with 60% to 70% of the molecules being eliminated in the first hour following injection and the remaining presenting with a half-life ranging from 9.5 to 15.5 hours (Figure 6A). In order to decipher the possible contribution of the binding to FcRn at neutral pH to the half-life of Fc-fused FVIII without the interference of endogenous VWF, we further compared the half-lives of rFVIII^Q and FVIII^{C1C2}Fc in VWF-KO mice. In the absence of endogenous VWF, FVIII^{C1C2}Fc demonstrated a 2.5-fold longer half-life (2.31 hours) than rFVIII^Q (0.94 hours; Figure 6B).

Discussion

Our work demonstrates the binding of rFVIII^Q to FcRn at neutral pH. Because FVIII alone exhibited weak binding affinity for FcRn by ELISA, and because some human IgG1 were documented to bind FcRn at pH 7.4 (see references^{36,37} and patent WO2013046704A2), we hypothesize that the binding of rFVIII^Q to FcRn at neutral pH results from a synergy between the weak binding affinities of the FVIII and Fc moieties of the molecule that leads to consistent augmentation in the binding avidity. The experimental data suggest that the interaction of rFVIII^Q with FcRn is relying on positively charged amino acids residues located in the C1 and/or C2 domains of FVIII. Indeed, reduction of the positive electrostatic potential of C1C2 by mutation of a few key amino acids was associated with a drastically reduced binding of rFVIII^Q to FcRn at neutral pH and with a statistically relevant increase in circulating half-life of Fc-fused FVIII in VWF-KO mice. Identifying the amino acid residue(s) that contribute(s) the most to FcRn binding would require generating individual

Table 2. Hydrogen bonds and salt bridges in the interaction of FVIII C1C2 domains and FcRn.

Residues in C1C2 domains	Residues in FcRn	Distance (Å)	FVIII domain
Hydrogen bonds			
C2021	N55	2.49	C1
R2090	S181	2.97	C1
R2090	P180	2.92	C1
K2207	D101	3.01	C2
Salt bridges			
E2181	R171	1.63	C2
K2207	D101	3.01	C2

Fc: “constant” crystallizable fragment; FcRn: neonatal Fc receptor; FVIII: coagulation factor VIII.

FVIII^{R2090A}Fc, FVIII^{K2092A}Fc or FVIII^{R2215A}Fc variants. More than ten therapeutic proteins with Food and Drug Administration authorization exploit the Fc-fusion technology for half-life extension.³⁸ Among these, procoagulant FVIII, which has an intrinsic mean physiological half-life of about 11 h,¹⁰ is among the Fc-fused therapeutic proteins with the lowest gain in half-life extension, i.e., 19 h.¹⁵ This value is significantly lower than that reach by other Fc-fused proteins such as rFIX^Q (i.e., 82 h),¹⁶ the extracellular domain of TNFR fused to Fc (i.e., 70 h),³⁹ Fc-fused CTLA-4 (i.e., 13 days)⁷ or therapeutic IgG1 antibodies (i.e., 21 days).⁴⁰ Binding of rFVIII^Q to endogenous VWF in the patients’ circulation has been identified as a key limitation for its duration in plasma, wherein elimination of the rFVIII^Q/VWF complexes by VWF-specific catabolic pathways imposes a glass ceiling on half-life extension.²⁵ In this respect, our finding of an interaction of the FVIII light chain of rFVIII^Q with FcRn at neutral pH represents a different molecular mechanism responsible for its limited extension of circulating time in plasma in addition to VWF-mediated mechanism. Our modeling results confirm a strong positive electrostatic potential of the FVIII C1 and C2 domains, and to a lesser extent of the FVIII A3 domain, and a key role of positively charged amino-acids in establishing contacts with FcRn. The binding of FVIII to the D'D3 domain of VWF implicates both the C1 domain and the acidic a3 peptide through a sulfated tyrosine, while the A3 and C2 domains play ancillary roles

present with negligible circulating FVIII levels owing to the lack of VWF or presence of dysfunctional VWF.^{46,47} Whether VWF also shields FVIII intracellularly is unclear. Sorvillo et al. demonstrated that, in contrast to FVIII, VWF is not or poorly endocytosed by human monocyte-derived dendritic cells.⁴⁸ Several endocytic receptors for VWF have however been identified on endothelial cells, including C-type lectin domain family 4 member M (CLEC4M), stabilin-2, and scavenger receptor class A member 5 (SCARA5),⁴⁹ some of which mediate the internalization of the FVIII-VWF complex. The possibility thus exists that VWF also participates in enhancing the FcRn-mediated intracellular recycling of rFVIII¹Fc by quenching its positively charged C1 and C2 domains in the endosome and preventing the interaction of C1C2 with FcRn. Indeed, the VWF/FVIII interaction is stable at pH >5.5, at least *in vitro*.⁵⁰

Our modeling of the electrostatic potential of FVIII domains indicated that the positive electrostatic potential of the light chain spreads to part of the A3 domain that is also protected by the D'D3 domain of VWF.⁴¹ In line with this, efanesoctocog α is a recently developed engineered Fc-fused FVIII in complex with the D'D3 domain of VWF with a half-life of 25–31 h in mice²⁵ and 33–45 h in the human.⁵¹ However, the optimal half-life of efanesoctocog α was not reached by the mere addition of the D'D3 domain of VWF, but required the grafting of XTEN polypeptides.²⁵ At neutral pH, rFVIII¹C2Fc retained a significant binding to FcRn *in vitro*, suggesting the participation of additional positive charges outside the C domains on FVIII in FcRn interaction. Whether the XTEN polypeptides shield additional positive charges, particularly at the interface between A2 and A3, that are not protected by the D'D3 domain of VWF, and prevent engagement with intracellular receptors, remains to be investigated.

The gain in half-life of rFVIII¹C2Fc as compared to rFVIII¹Fc (from 56 to 138 minutes; Figure 6B) was only evidenced in the absence of endogenous VWF. Performing similar experiments in transgenic VWF-KO mice expressing the human instead of mouse FcRn may yield more pre-clinically relevant results.⁵² Yet, the findings are reminiscent of our previous observation that an increase in half-life from 17 to 41 minutes of the individual FVIII¹C1 and FVIII¹C2 variants was only observed in the absence of endogenous VWF.³³ Interestingly, our previous work showed a reduction in FVIII immunogenicity when the charged residues in the C1 domain of FVIII were mutated. However, once again, this was observed in the absence of endogenous VWF.³³ Whether the reduction of the positive electrostatic potential may be an advantage in the context of FVIII synthesis and intracellular trafficking, where VWF is not at play, needs to be investigated.

In conclusion, we describe an additional mechanism to the VWF-mediated catabolism of rFVIII¹Fc (Online Supplementary Figure S5). The predominant role played by VWF on FVIII catabolism however puts in perspective our find-

ings in terms of translational possibilities. In addition, our attempt to disfavor FVIII binding to FcRn at physiological pH also marginally affected binding to VWF and reduced the specific activity of the molecule, possibly by altering binding to phospholipids. Nonetheless, our data open a mutational space for the reduction of the positive electrostatic potential of rFVIII¹Fc, to limit its interactions with molecules that favor its catabolism or prevent its recycling. Besides, complementary strategies may be foreseen to further optimize the half-life of Fc-fused FVIII. For instance, Fc-engineering by introducing the YTE substitutions to strengthen human FcRn interactions was shown to extend the half-life of mAb with positively charged patches in the Fab fragments.¹⁹ Whether the same strategy may apply to rFVIII¹Fc, efanesoctocog α , or rFVIII¹C2Fc, remains to be determined. Importantly, beyond the mere example of FVIII, our finding may also be of interest for therapeutic proteins that bear patches with positive net charges and exhibit poor pharmacokinetics.

Disclosures

SLD is co-inventor in two patents related to Fc-fused proteins (US20220175896A1 and US20170072032A1). The other authors have no conflict of interest to disclose.

Contributions

ARR, SD, ASB, KV, JDD and SLD designed the research. ARR, SD, ASB and LD performed the experiments. OC, SJ and RL contributed essential material. ARR, SD, ASB, KV, JDD and SLD analyzed the results. ARR, SD, ASB and SLD wrote the manuscript.

Acknowledgments

ReFacto® and Eloctate® were kind gifts from Novo Nordisk A/S (Måløv, Denmark), and Sanofi-Genzyme (Cambridge, MA)/Swedish Orphan Biovitrum AB (Stockholm, Sweden). We thank to Hugo Mouquet (Institut Pasteur, France), for providing the genes encoding the VL and VH regions of human anti-HIV m66.6 IgG, as well as the staff from “Centre d’Expérimentation Fonctionnelle” and “Centre d’Histologie, d’Imagerie Cellulaire et de Cytométrie (CHIC)”, a member of the Sorbonne Université Cell Imaging and Flow Cytometry network (LUMIC) and UPD cell imaging networks, at Centre de Recherche des Cordeliers (Paris) for assistance.

Funding

This work was supported by Institut National de la Santé et de la Recherche Médicale (INSERM), Centre National de la Recherche Scientifique (CNRS), Sorbonne Université, Université de Paris, Assistance Publique des Hôpitaux de Paris and funded by the European Union’s Horizon 2020 research and innovation program under the Marie Skłodowska-Curie grant agreement n°859974 (EDUC8) and by grants from Agence National de la Recherche (ANR-18-CE17-0010-02, n°18181LL, Exfiltrins), Sanofi-Genentech (Waltham, MA) and

(Swedish Orphan Biovitrum AB (Höllviksnäs, Sweden). ARR was the recipient of fellowships from MSCA-ITN EDUC8 (n°859974) and from FRM (FDT202304016725). KV acknowledges the receipt of VTT International Research Found (ref no. VIN/2022-23/011 dated February 9, 2023).

Data-sharing statement

All data are included in the paper or in the Online Supplementary Appendix. Additional data will be shared on reasonable request to the corresponding author.

References

1. Spiegelberg HL, Fishkin BG, Grey HM. Catabolism of human gammaG-immunoglobulins of different heavy chain subclasses. I. Catabolism of gammaG-myeloma proteins in man. *J Clin Invest.* 1968;47(10):2323-2330.
2. Challacombe SJ, Russell MW. Estimation of the intravascular half-lives of normal rhesus monkey IgG, IgA and IgM. *Immunology.* 1979;36(2):331-338.
3. Waldmann TA, Strober W. Metabolism of immunoglobulins. *Prog Allergy.* 1969;13:1-110.
4. Blumberg LJ, Humphries JE, Jones SD, et al. Blocking FcRn in humans reduces circulating IgG levels and inhibits IgG immune complex-mediated immune responses. *Sci Adv.* 2019;5(12):eaax9586.
5. Martin WL, West AP, Gan L, Bjorkman PJ. Crystal structure at 2.8 Å of an FcRn/heterodimeric Fc complex: mechanism of pH-dependent binding. *Mol Cell.* 2001;7(4):867-877.
6. Pyzik M, Kozicky LK, Gandhi AK, Blumberg RS. The therapeutic age of the neonatal Fc receptor. *Nat Rev Immunol.* 2023;23(7):415-432.
7. Lutt J. Efficacy, safety, and tolerability of abatacept in the management of rheumatoid arthritis. *Open Access Rheumatol.* 2009;1:17-35.
8. Shen J, Townsend R, You X, et al. Pharmacokinetics, pharmacodynamics, and immunogenicity of belatacept in adult kidney transplant recipients. *Clin Drug Investig.* 2014;34(2):117-126.
9. Ipema HJ, Jung MY, Lodolce AE. Romiplostim management of immune thrombocytopenic purpura. *Ann Pharmacother.* 2009;43(5):914-919.
10. Versloot O, Iserman E, Chelle P, et al. Terminal half-life of FVIII and FIX according to age, blood group and concentrate type: data from the WAPPS database. *J Thromb Haemost.* 2021;19(8):1896-1906.
11. Srivastava A, Santagostino E, Dougall A, et al. WFH guidelines for the management of hemophilia, 3rd edition. *Haemophilia.* 2020;26(Suppl 6):1-158.
12. Konkle BA, Stasyshyn O, Chowdary P, et al. Pegylated, full-length, recombinant factor VIII for prophylactic and on-demand treatment of severe hemophilia A. *Blood.* 2015;126(9):1078-1085.
13. Escuriola Ettingshausen C, Hegemann I, Simpson ML, et al. Favorable pharmacokinetics in hemophilia B for nonacog beta pegol versus recombinant factor IX-Fc fusion protein: a randomized trial. *Res Pract Thromb Haemost.* 2019;3(2):268-276.
14. Chia J, Louber J, Glauser I, et al. Half-life-extended recombinant coagulation factor IX-albumin fusion protein is recycled via the FcRn-mediated pathway. *J Biol Chem.* 2018;293(17):6363-6373.
15. Mahlangu J, Powell JS, Ragni MV, et al. Phase 3 study of recombinant factor VIII Fc fusion protein in severe hemophilia A. *Blood.* 2014;123(3):317-325.
16. Powell JS, Pasi KJ, Ragni MV, et al. Phase 3 study of recombinant factor IX Fc fusion protein in hemophilia B. *N Engl J Med.* 2013;369(24):2313-2323.
17. Igawa T, Tsunoda H, Tachibana T, et al. Reduced elimination of IgG antibodies by engineering the variable region. *Protein Eng Des Sel.* 2010;23(5):385-392.
18. Schoch A, Kettenberger H, Mundigl O, et al. Charge-mediated influence of the antibody variable domain on FcRn-dependent pharmacokinetics. *Proc Natl Acad Sci U S A.* 2015;112(19):5997-6002.
19. Grevys A, Frick R, Mester S, et al. Antibody variable sequences have a pronounced effect on cellular transport and plasma half-life. *iScience.* 2022;25(2):103746.
20. Pipe SW, Montgomery RR, Pratt KP, Lenting PJ, Lillicrap D. Life in the shadow of a dominant partner: the FVIII-VWF association and its clinical implications for hemophilia A. *Blood.* 2016;128(16):2007-2016.
21. Fay PJ, Coumans JV, Walker FJ. von Willebrand factor mediates protection of factor VIII from activated protein C-catalyzed inactivation. *J Biol Chem.* 1991;266(4):2172-2177.
22. Pegon JN, Kurdi M, Casari C, et al. Factor VIII and von Willebrand factor are ligands for the carbohydrate-receptor Siglec-5. *Haematologica.* 2012;97(12):1855-1863.
23. Nogami K, Shima M, Nishiya K, et al. A novel mechanism of factor VIII protection by von Willebrand factor from activated protein C-catalyzed inactivation. *Blood.* 2002;99(11):3993-3998.
24. Swystun LL, Lai JD, Notley C, et al. The endothelial cell receptor stabilin-2 regulates VWF-FVIII complex half-life and immunogenicity. *J Clin Invest.* 2018;128(9):4057-4073.
25. Chhabra ES, Liu T, Kulman J, et al. BIVV001, a new class of factor VIII replacement for hemophilia A that is independent of von Willebrand factor in primates and mice. *Blood.* 2020;135(17):1484-1496.
26. Zhu Z, Qin HR, Chen W, et al. Cross-reactive HIV-1-neutralizing human monoclonal antibodies identified from a patient with 2F5-like antibodies. *J Virol.* 2011;85(21):11401-11408.
27. Ducore JM, Miguelino MG, Powell JS. Alprolix (recombinant Factor IX Fc fusion protein): extended half-life product for the prophylaxis and treatment of hemophilia B. *Expert Rev Hematol.* 2014;7(5):559-571.
28. Ledgerwood JE, Coates EE, Yamshchikov G, et al. Safety, pharmacokinetics and neutralization of the broadly neutralizing HIV-1 human monoclonal antibody VRC01 in healthy adults. *Clin Exp Immunol.* 2015;182(3):289-301.
29. Lenting PJ, Van Mourik JA, Mertens K. The life cycle of coagulation factor VIII in view of its structure and function. *Blood.* 1998;92(11):3983-3996.
30. van den Brink EN, Turenhout EA, Bovenschen N, et al. Multiple VH genes are used to assemble human antibodies directed toward the A3-C1 domains of factor VIII. *Blood.* 2001;97(4):966-972.
31. Jacquemin MG, Desqueper BG, Benhida A, et al. Mechanism and kinetics of factor VIII inactivation: study with an IgG4 monoclonal antibody derived from a hemophilia A patient with inhibitor. *Blood.* 1998;92(2):496-506.
32. Wroblewska A, van Haren SD, Herczenik E, et al. Modification of

- an exposed loop in the C1 domain reduces immune responses to factor VIII in hemophilia A mice. *Blood*. 2012;119(22):5294-5300.
33. Gangadharan B, Ing M, Delignat S, et al. The C1 and C2 domains of blood coagulation factor VIII mediate its endocytosis by dendritic cells. *Haematologica*. 2017;102(2):271-281.
 34. Sand KMK, Dalhus B, Christianson GJ, et al. Dissection of the neonatal Fc receptor (FcRn)-albumin interface using mutagenesis and anti-FcRn albumin-blocking antibodies. *J Biol Chem*. 2014;289(24):17228-17239.
 35. Delignat S, Reyes J, Dasgupta S, et al. Removal of mannose-ending glycan at Asn2118 abrogates FVIII presentation by human monocyte-derived dendritic cells. *Front Immunol*. 2020;11:393.
 36. Dumet C, Pugnière M, Henriquet C, Gouilleux-Gruart V, Poupon A, Watier H. Harnessing Fc/FcRn affinity data from patents with different machine learning methods. *Int J Mol Sci*. 2023;24(6):5724.
 37. Rossini S, Noé R, Daventure V, Lecerf M, Justesen S, Dimitrov JD. V Region of IgG controls the molecular properties of the binding site for neonatal Fc receptor. *J Immunol*. 2020;205(10):2850-2860.
 38. Duivelshof BL, Murisier A, Camperi J, et al. Therapeutic Fc-fusion proteins: current analytical strategies. *J Sep Sci*. 2021;44(1):35-62.
 39. Nestorov I, Zitnik R, DeVries T, Nakanishi AM, Wang A, Banfield C. Pharmacokinetics of subcutaneously administered etanercept in subjects with psoriasis. *Br J Clin Pharma*. 2006;62(4):435-445.
 40. Ko S, Jo M, Jung ST. Recent achievements and challenges in prolonging the serum half-lives of therapeutic IgG antibodies through Fc engineering. *BioDrugs*. 2021;35(2):147-157.
 41. Chiu P-L, Bou-Assaf GM, Chhabra ES, et al. Mapping the interaction between factor VIII and von Willebrand factor by electron microscopy and mass spectrometry. *Blood*. 2015;126(8):935-938.
 42. Panteleev MA, Ananyeva NM, Greco NJ, Ataullakhanov FI, Saenko EL. Factor VIIIa regulates substrate delivery to the intrinsic factor X-activating complex. *FEBS J*. 2006;273(2):374-387.
 43. Meeks SL, Healey JF, Parker ET, Barrow RT, Lollar P. Antihuman factor VIII C2 domain antibodies in hemophilia A mice recognize a functionally complex continuous spectrum of epitopes dominated by inhibitors of factor VIII activation. *Blood*. 2007;110(13):4234-4242.
 44. Batsuli G, Deng W, Healey JF, et al. High-affinity, noninhibitory pathogenic C1 domain antibodies are present in patients with hemophilia A and inhibitors. *Blood*. 2016;128(16):2055-2067.
 45. Weflen AW, Baier N, Tang Q-J, et al. Multivalent immune complexes divert FcRn to lysosomes by exclusion from recycling sorting tubules. *Mol Biol Cell*. 2013;24(15):2398-2405.
 46. Mazurier C, Goudemand J, Hilbert L, Caron C, Fressinaud E, Meyer D. Type 2N von Willebrand disease: clinical manifestations, pathophysiology, laboratory diagnosis and molecular biology. *Best Pract Res Clin Haematol*. 2001;14(2):337-347.
 47. Adjambri AE, Bouvier S, N'guessan R, et al. Discovery of Type 3 von Willebrand disease in a cohort of patients with suspected hemophilia A in Côte d'Ivoire. *Mediterr J Hematol Infect Dis*. 2020;12(1):e2020019.
 48. Sorvillo N, Hartholt RB, Bloem E, et al. Von Willebrand factor binds to the surface of dendritic cells and modulates peptide presentation of factor VIII. *Haematologica*. 2016;101(3):309-318.
 49. Swystun LL, Lillicrap D. Current understanding of inherited modifiers of FVIII pharmacokinetic variation. *Pharmgenomics Pers Med*. 2023;16:239-252.
 50. Dimitrov JD, Christophe OD, Kang J, et al. Thermodynamic analysis of the interaction of factor VIII with von Willebrand factor. *Biochemistry*. 2012;51(20):4108-4116.
 51. Konkle BA, Shapiro AD, Quon DV, et al. BIVV001 fusion protein as factor VIII replacement therapy for hemophilia A. *N Engl J Med*. 2020;383(11):1018-1027.
 52. Roopenian DC, Christianson GJ, Sproule TJ. Human FcRn transgenic mice for pharmacokinetic evaluation of therapeutic antibodies. *Methods Mol Biol*. 2010;602:93-104.